PHOTON NOISE IN THE SIS DETECTOR

Noshir B. Dubash, Gordana Pance, Michael J. Wengler
Electrical Engineering
University of Rochester, Rochester, NY 14627

Abstract

The dominant source of noise in an SIS mixer is the noise in the photon-induced dc current. We have made accurate measurements of noise induced in SIS junctions by 95 GHz photons. The noise in the dc current was measured at 1.5 GHz using a low-noise cryogenic measurement system. Noise measurements have been made on single $Nb/AlO_x/Nb$ junctions which are poorly coupled to the radiation due to their large parasitic capacitance. Noise in these SIS's is nearly perfectly predicted by Tucker's theory augmented by a vacuum/thermal noise term. Measurements of series arrays of these junctions also agree with this theory showing that the noise of each SIS in the array is independent. We have also measured SIS's which are well coupled to the radiation because of integrated tuning structures. The photon induced noise in these SIS's deviated significantly from theoretical predictions. We do not yet have an explanation or an alternate theory for this case.

I. Introduction

For small rf power, on the first photon step, the superconductor-insulator-superconductor (SIS) diode should behave as a photodiode and the noise in the photon-induced current should be equal to shot noise [1]. At higher rf power, and at dc bias other than on the first photon step, Tucker's theory [2] augmented by the vacuum noise term proposed by Wengler and Woody [3] must be used to predict the noise in the photon induced current. The predictions of Tucker's theory are based on a detailed microscopic theory of electronic states, and electron tunneling in the presence of radiation. Thus the measurement of this noise provides a detailed insight into the mechanism of current transport across the SIS.

Accurate measurement of SIS mixer noise have been made by several groups [4-6]. These measurements have provided valuable information about receiver sensitivity. The noise reported is often larger than that predicted by Tucker's theory. It is also difficult to determine if the excess mixer noise temperature is due to a lower mixer gain or a higher than expected noise at the mixer output.

We have chosen to make direct measurements of photon noise by injecting the photons through a cold 4.2 K attenuator to eliminate the thermal background. Our measurements of noise
can now be directly related to the statistics of the photon absorption process in the SIS. For instance, we can confirm that some SIS's have photon induced shot noise on their first photon step, and we can see how that shot noise saturates at higher photon fluxes. These measurements will lead to a better understanding of the fundamental processes that limit the sensitivity of the SIS mixer.

II. Experimental Set-up and Measurement Technique

To make calibrated measurements of available noise power at the SIS we need: 1) a low-noise and high-gain amplification system, 2) a way to accurately measure the gain and noise of this system, and 3) a way to measure the reflection coefficient at the SIS. Such a system has been designed and built. Our system uses noise measurement techniques developed by McGrath *et al.* [7] and is similar to one described by Pan *et al.* [8]. A schematic diagram of the measurement system is shown in figure 1. The high gain is provided by an ultra-low-noise HEMT amplifier. The temperature loads are used to calibrate the gain and noise of the system. The reflection coefficient is determined by injecting an external noise signal through the circulator, which can be reflected off the SIS or the short. The coaxial switch is used to switch to the temperature loads for the gain and noise calibration, and between the short and the SIS in the reflection coefficient measurement. All the microwave components in the system are optimized to operate in a 400 MHz bandwidth centered at 1.5 GHz. All noise measurements reported in this paper were made in this bandwidth. The SIS block consists of the SIS mounted in a 4.2 K cavity, and the bias tee which enables the dc biasing and capacitively couples the 1.5 GHz output. The SIS block has the capability of being temperature controlled up to 20 K for measurements above the superconducting transition temperature, and Johnson noise calibration.

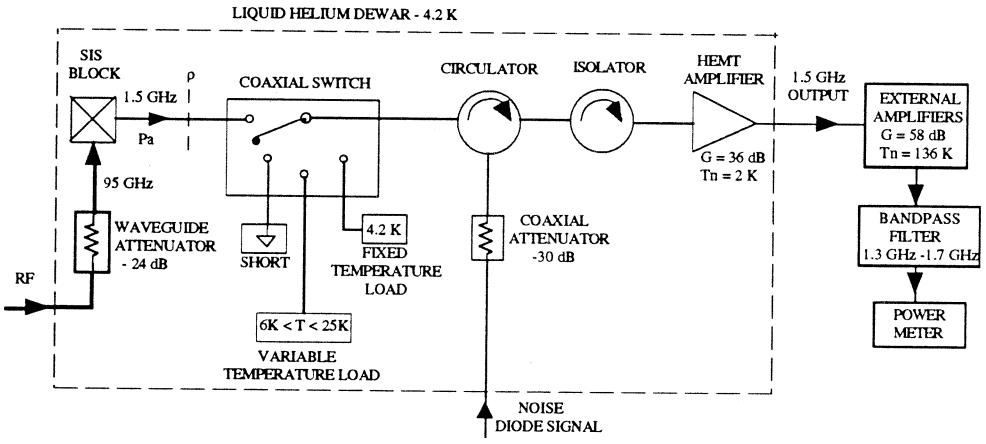

Figure 1 Schematic diagram of low-noise 1.5 GHz cryogenic measurement system

The circulator and isolator together provide 40 dB of isolation between the SIS and the HEMT amplifier. This level of isolation was found to be necessary to provide accurate measurements when the SIS was poorly matched to the amplifier. Noise waves from the input of the amplifier get reflected off the SIS and add coherently to the amplifier noise, thus increasing the effective system noise. This increase would not be detected in the calibration with the matched temperature loads.

We also measure the loss between the coaxial switch and the SIS, which is primarily the loss in the bias tee. This loss is measured by reflecting the noise signal off the SIS biased on the supercurrent. The reflected power is then compared to the power reflected off the short. If there is no series resistance in the supercurrent the SIS should look like a perfect short when current biased on the supercurrent. The noise signal must not be large enough to switch the SIS into the voltage state. The loss measured using this method is typically about 0.2 dB.

The system noise and gain is calibrated by measuring the output power for several load temperatures between 6 and 15 K. These data points are then fitted to a straight line to obtain the gain and noise of the system. The fitting error is typically less than 0.1%. The gain and noise temperature of the system measured at 4.2 K is typically 94.80 dB and 4.38 K respectively. We estimate the accuracy of the noise temperature measurement to be 0.1 to 0.4 K. The added noise power due to the loss in the stainless steel coaxial cable connecting the load to the coaxial switch is included in the calibration.

We need to determine the *available* noise power in the SIS at 1.5 GHz. Due to reflection and transmission loss we cannot successfully couple all the available power out of the SIS. The calibration of the system gain and noise allows us to measure the power successfully coupled out of the SIS. Using the measured loss and reflection coefficient we can then determine what the available power at the SIS was. The available output power P_a at the SIS is then given by

$$P_a = \frac{(P_{out} - \rho P_0)/G - P_n(1-\rho) - P_{eff}(\rho + t)}{(t - \rho/t)} \qquad (1)$$

where P_{out} is the SIS output measured on the power meter. P_0 corresponds to the power from the cold attenuator connected to the circulator, G and P_n are the measured gain and noise power of the system respectively, ρ is the measured power reflection coefficient at the SIS, t is power transmission coefficient of the measured loss, and P_{eff} is the effective noise power of the loss.

The measured loss is treated as a matched attenuation at the temperature of the SIS block. The noise added by the insertion loss of the isolator and circulator at 4.2 K is included in the system noise obtained from the calibration. The percentage error in the measurement of P_a will in general depend on the impedance of the SIS since the error in the reflection coefficient is magnified at larger values of reflection coefficient because of the very small powers that can be coupled out of the SIS. Since the directivity of the circulator is 20 dB the accuracy in the measurement of the reflection coefficient is at best 1%. Including all other random and systematic losses we estimate the accuracy in P_a to be between 1% and 5% for impedances between 3 Ω and 1000 Ω. This level of accuracy has been verified using an unbiased SIS above its superconducting transition temperature as a Johnson noise source.

The 95.5 GHz rf enters the dewar through a WR-10 waveguide port. It is then injected through a 24 dB waveguide attenuator which is cooled to 4.2 K. The attenuator consists of a nichrome-coated vane which is inserted into the broad side of the WR-10 waveguide. The vane is well heat sunk to 4.2 K. Treating this as a matched attenuator with 295 K at the input, the thermal radiation at the output of the attenuator is estimated to be 5.1 K.

The SIS output power P_a can also be expressed as an equivalent temperature using the Rayleigh-Jeans law: $P_a = kT_aB$. B is the bandwidth in which P_a is measured and k is Boltzmann's constant. We use this presentation when measuring P_a from an SIS above its superconducting transition temperature. With no dc bias on it, this SIS is a Johnson noise source with T_a equal to the actual physical temperature of the SIS. These measurements are used to verify the accuracy of our measurement system, and are described below.

We will most often express the noise in units of current. A noise source can be represented by an ideal noise current generator shunted by R_d, the dynamic impedance of the noise source. The noise current generator that would produce power P_a has mean square value $\langle i^2 \rangle = 4 P_a / R_d$, where R_d is the dynamic impedance of the SIS. The dynamic resistance R_d is determined by modulating the dc bias with a small ac voltage signal at 200 Hz, and detecting the current response with a lock-in amplifier.

The measured noise expressed as a current that we use is

$$\frac{\langle i^2 \rangle}{2eB} = \frac{2P_a}{eBR_d} \qquad (2)$$

The point of expressing noise in this way is to allow easy comparison with shot noise. If a dc current I_0 generates shot noise, then its equivalent noise current generator has $\langle i^2 \rangle = 2eI_0B$. If the SIS whose output noise we are measuring is behaving as an ideal shot noise source, then a comparison of $\langle i^2 \rangle/2eB$ with the SIS's dc current I_0 will find them identical. As theory predicts, and our measurements show, the SIS is operating as a perfect shot noise source under many circumstances.

III. Junction Description

The junctions tested were fabricated at Hypres and at IBM. The Hypres junctions come from their all-refractory niobium tri-layer process. These $Nb/AlO_x/Nb$ junctions have an area of 11 μm^2, specific capacitance of 38 $fF/\mu m^2$, and current density of about 950 A/cm^2. The normal resistance is about 22 Ω and the ωR_nC product at 95.5 GHz is about 5.5. The junctions in the series arrays are identical to the single junction. All junctions and arrays were fabricated at the center of a self complimentary log-periodic antenna which has an impedance of 75 Ω on the silicon substrate. These junctions were poorly coupled to the 95.5 GHz rf radiation due to their large area and hence large parasitic capacitance. This capacitance can be tuned out using integrated tuning circuits. We tested a single junction with a tuning circuit. The tuning circuit consists of an inductive section that tunes out the junction capacitance, and a quarter-wavelength microstripline transformer that matches the rf resistance of the junction to the antenna [9].

We also tested a $Nb/AlO_x/Nb$ junction that was fabricated at IBM. This junction had an area of ~ 4 μm^2, specific capacitance of ~ 50 $fF/\mu m^2$, and current density of ~ 2400 A/cm^2. The normal resistance was 21.2 Ω, giving an ωR_nC product of about 2.7 at 95.5 GHz. The junction was fabricated at the center of the same 75 Ω log-periodic antenna, and had a similar integrated tuning circuit as the one described above.

IV. Experimental Results and Analysis

A. Noise measurements with no rf power and a 4.2 K background

(i) NIN measurement and Johnson noise calibration

For this measurement the SIS block was heated above the superconducting transition of the niobium SIS junction, and maintained at a temperature of 10.79 K using a temperature controller. At this temperature, the SIS becomes a Normal-metal-Insulator-Normal-metal (NIN) junction. While an SIS is highly non-linear, the NIN provides an ohmic IV curve. At zero voltage bias, the NIN is a perfect Johnson noise source while at high voltage bias the NIN approaches a perfect shot noise source.

In the NIN measurement, there are losses in the niobium circuit that are negligible below the superconducting transition temperature. These losses can not be measured by the method described in section II, which involves reflecting a noise signal off the SIS biased on the supercurrent. There is a series resistance of about 2.2 Ω due to the resistance of the niobium thin film antenna leads in the normal state. This resistance acts as an additional loss between the SIS and the coaxial switch. There is also loss due to the heating of the stainless steel coaxial cable connecting the SIS to the coaxial switch. The total loss was calculated by comparing the

measured reflection coefficient off the NIN to that expected from its normal resistance matching to the load resistance. This loss was then calibrated out of the measurement. There was also a thermal gradient of 0.71 K between the temperature sensor and the SIS. This was calculated by recording the temperature at which the antenna leads went superconducting, and comparing that to the transition temperature for Niobium.

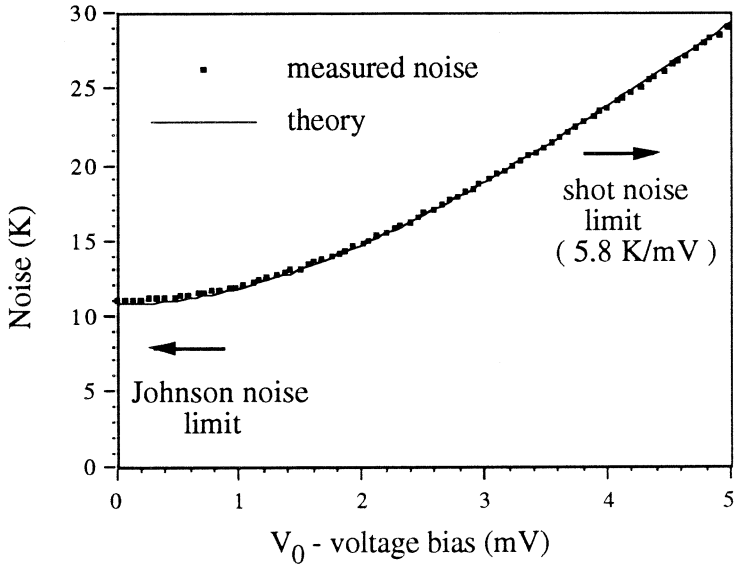

Figure 2 Measured and theoretical noise for a single niobium tunnel junction in its NIN state at a temperature of 10.79 K. The theory is calculated from the fluctuation dissipation relation of equation 4.

Figure 2 shows the measured noise compared to the theoretical noise in an NIN tunnel junction. The theoretical noise is calculated from the fluctuation dissipation relation derived by Rogovin and Scalapino [10]. The mean-square current noise or fluctuation for an NIN tunnel junction is given by:

$$\left\langle i_n^2 \right\rangle = 2e \frac{V_0}{R_n} B \coth\left[\frac{eV_0}{2kT}\right] \tag{3}$$

where V_0 is the dc voltage bias, R_n is the normal resistance, B is the bandwidth of the measurement, and T is the ambient temperature. This noise can be expressed as a temperature T_n using the Rayleigh-Jeans law.

$$T_n = \frac{eV_0}{2k} \coth\left[\frac{eV_0}{2kT}\right] \tag{4}$$

The measured noise agrees very well with this theoretical hyperbolic cotangent function. For very small V_0, $\coth(eV_0/2kT) \approx 2kT/eV_0$, and T_n is equal to the ambient temperature T, which corresponds to Johnson noise. At large V_0 the hyperbolic cotangent approaches unity and T_n approaches shot noise given by $T_{shot} = eV_0/2k = 5.8$ K/mV.

The bias was then turned off and the NIN junction was further heated and the power measured for several temperatures between 10 K and 15 K. The unbiased NIN behaves as a resistor which allows us to calibrate our system with Johnson noise. The measured noise was within 3 % of the theoretical Johnson noise.

(ii) SIS single junctions

We measured the noise in three SIS junctions with no rf power: the Hypres single junction, the Hypres single junction with the tuning circuit, and the IBM junction with the tuning circuit. Figure 3 shows the noise measured for two of these junctions. Since the measured noise is plotted as $\langle i^2 \rangle / 2eB$, the equivalent shot noise is then simply given by the dc IV curve. Tucker's theory predicts that SIS junctions with no radiation present are perfect shot noise sources.

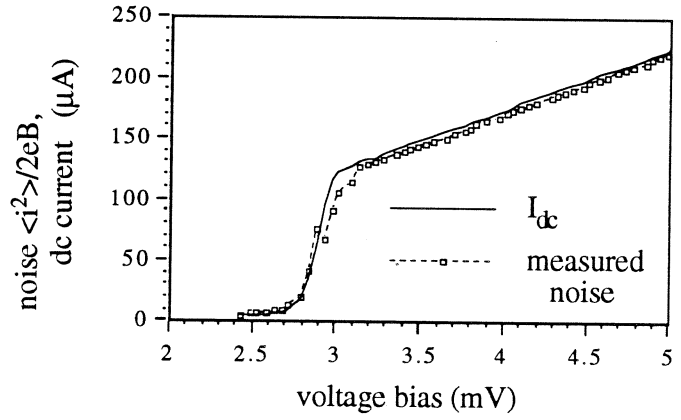

(a)

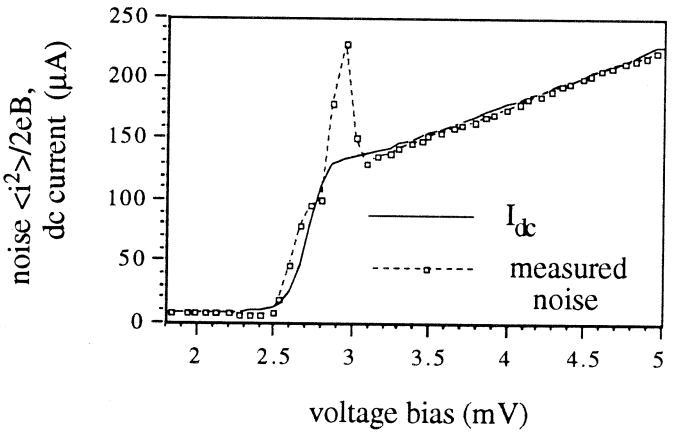

(b)

Figure 3 Measured noise in an SIS with no incident rf power for, (a) a single IBM junction, and (b) a single Hypres junction. The noise is expressed in units of current and may directly be compared to the measured dc current I_{dc} for comparison to shot noise.

In all three junctions the measured noise agreed very well with shot noise; in the leakage current region below the gap, and in the resistive region above the gap. We expected the noise in the resistive region to be equal to shot noise, but it was not clear that the noise in the leakage current should be shot noise, since the mechanism that leads to the leakage current is not well understood. We have verified that the leakage current is due to the independent tunneling of quasiparticles.

The peak that appears to be excess noise above the gap was consistently seen in all the Hypres junctions but was not seen in the IBM junction. Applied magnetic field partially suppressed this peak without affecting the noise elsewhere. This leads us to suggest the possibility that the excess noise might be due to some interaction of quasiparticles with Josephson currents.

(iii) Series arrays of SIS junctions

If the junctions in the array are identical and if the shot noise sources of the individual junctions are not correlated with each other, then the shot noise of the array is given by $\langle i^2 \rangle = 2eI_0B/N$ where N is the number of junctions in the array [11]. We measured two series arrays of two and four SIS junctions. In figure 4 we compare the measured noise $\langle i^2 \rangle/2eB$ to I_0/N. The measured noise fits the incoherent addition of noise exactly.

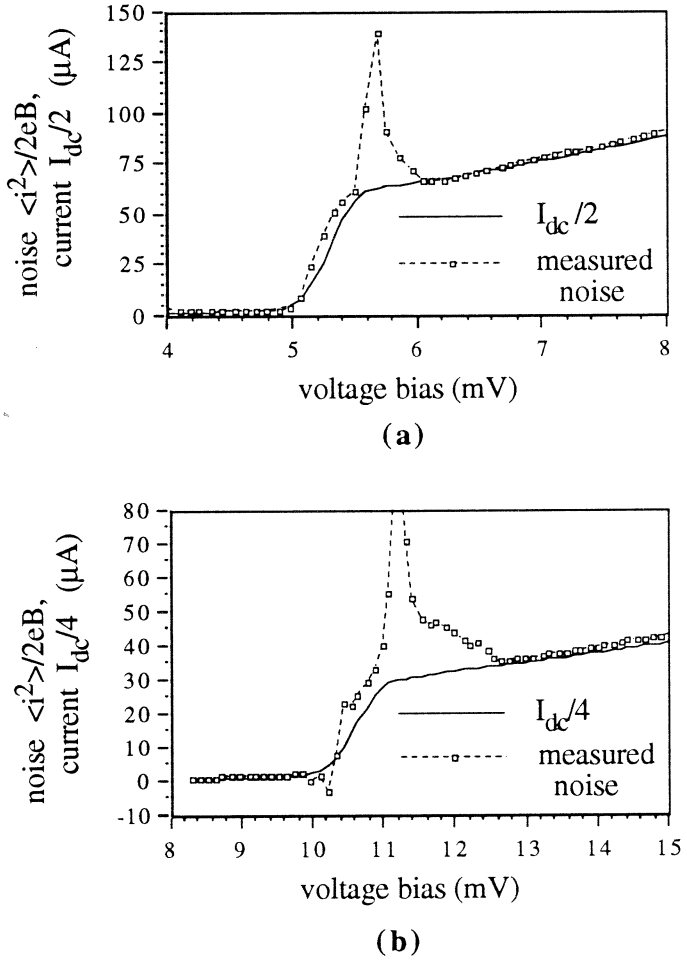

Figure 4 Measured noise in series arrays of SIS junctions with no incident rf power. (a) is a two junction array and (b) is a four junction array. Also plotted is the dc IV curve with the current scaled down by the number of junctions in the array.

On the linear part of the array IV curve at higher dc bias voltages, the available power has a slope of 5.8/N K/mV, expressed in terms of equivalent Rayleigh-Jeans temperature. This slope can be used for calibrating IF amplifier noise in SIS array mixers in a simple method described by Woody *et al* .[12].

Excess noise is detected above the gap as with the single junction. Applied magnetic field partially suppresses this noise as with the single junction.

B. Photon noise measurements: rf injection at 95.5 GHz and a 5.1 K background

Photon noise measurements were made for three single junctions and the four junction series array. Since the single junctions have different source impedances determined by the junction capacitance and the tuning structure, their measurements will be presented separately. Photon noise measurements were made as a function of dc bias voltage at a fixed rf power with $\alpha \approx 1$, and as a function of rf power biased on the middle of the first photon step. $\alpha = eV_{rf} / h\nu$ and will be referred to as the normalized rf voltage, where V_{rf} is the amplitude of the rf voltage at the SIS and ν is the rf frequency. For fixed external rf power, α will change as a function of dc bias on the SIS because the rf impedance of the SIS varies with dc bias.

The theoretical noise is calculated the using the three-port model of Tucker's theory [13], with the addition of the vacuum noise that arises from the quantization of the radiation field [3]. The total mean-sqaure current noise in the SIS can then be written as,

$$\langle i^2 \rangle = B \sum_{m,m'=-1}^{+1} \lambda_{0m} \lambda^*_{0m'} H_{mm'} + 4G_s \left|\lambda_{01}\right|^2 h\nu B \coth\left[\frac{h\nu}{2kT}\right] . \tag{5}$$

The first term is the noise predicted by Tucker's theory, where $H_{mm'}$ is the current correlation matrix. Expressions for $H_{mm'}$ and $|\lambda_{01}|^2$ for a three-port mixer model with the small IF approximation are given by Tucker and Feldman [2]. The second term represents the vacuum noise in the thermal background at temperature T. For our measurements T = 5.1 K, as explained in section II. $|\lambda_{01}|^2$ is related to the mixer gain. We assume the double sideband case, in which the upper sideband gain is equal to the lower sideband gain, which implies that $\lambda_{01} = \lambda_{0-1}$. G_s is the real part of the source admittance Y_s. The source admittance Y_s was determined from the antenna impedance, junction capacitance, and impedance of the tuning circuit, if any. The admittance obtained was fairly close to that obtained by curve fitting the theoretical pumped IV curve to the measured curve.

(i) Hypres single junction with no tuning circuit

The measured and theoretical noise for this junction as a function of dc bias are shown in figure 5. The rf power corresponds to $\alpha = 0.85$ at a dc bias of 2.45 mV. The measured noise shows good agreement with the theory below the gap voltage. Both the measured and theoretical noise do not deviate much from shot noise at biases below the gap voltage. However, the theory's deviation from shot noise on the first step at about 2.65 mV is maintained in the measurement. The comparisons to shot noise are made by comparison to the dc current I_0. There is some structure in the noise above the gap that is not predicted by the theory. This structure is partially suppressed by applied magnetic field.

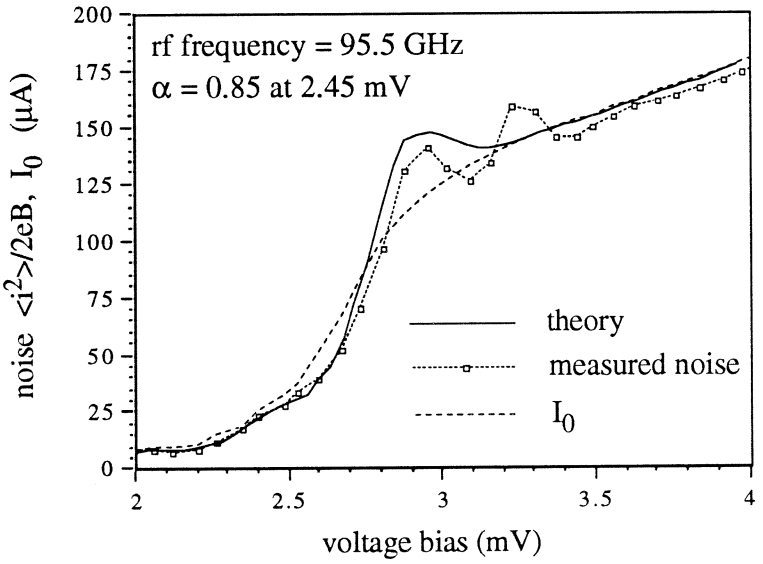

Figure 5 Photon-induced noise in a single Hypres junction as a function of dc bias voltage. The theory is calculated from Tucker's theory, including the contribution from vacuum noise. Also plotted is the measured dc current I_0 which includes the photon induced current. The dc IV curve, with no incident radiation, for this junction is shown in figure 3(b).

The noise as a function of the square of the normalized rf voltage is shown in figure 6. The SIS is biased on the first photon step at 2.45 mV. The measured noise is in good agreement with the theory, maintaining the same deviation from shot noise that the theory does. At low rf power the noise is exactly equal to shot noise as predicted by photodiode mixer theory [1].

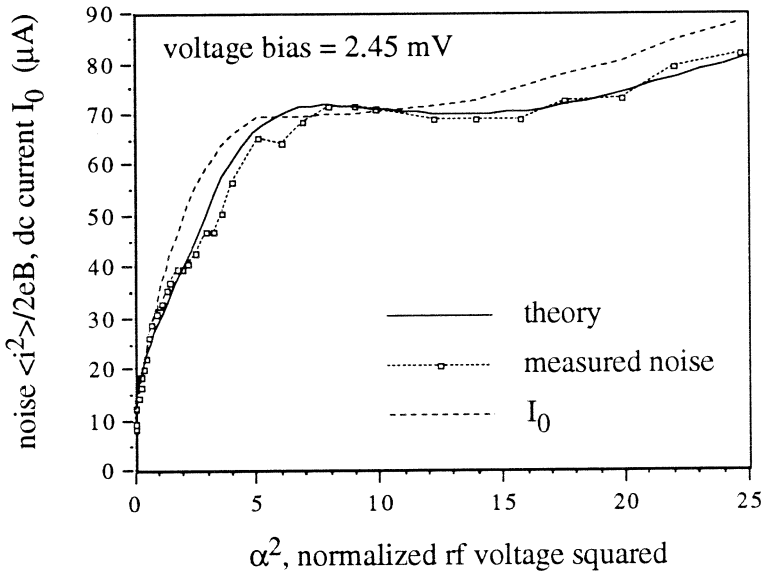

Figure 6 Photon-induced noise in the single Hypres SIS junction as a function of the normalized rf voltage squared. The junction was biased on the first photon step at 2.45 mV. Also shown is the measured dc current for comparison to shot noise.

(ii) Hypres four junction series array (no tuning circuit)

The noise measurements for the four junction array and the comparison to theory are illustrated in figures 7 and 8. The measurements agree very well with the theory except for region above the gap, and are very similar to the single junction measurements with the currents and voltages scaled appropriately. The theory was calculated using the "equivalent single

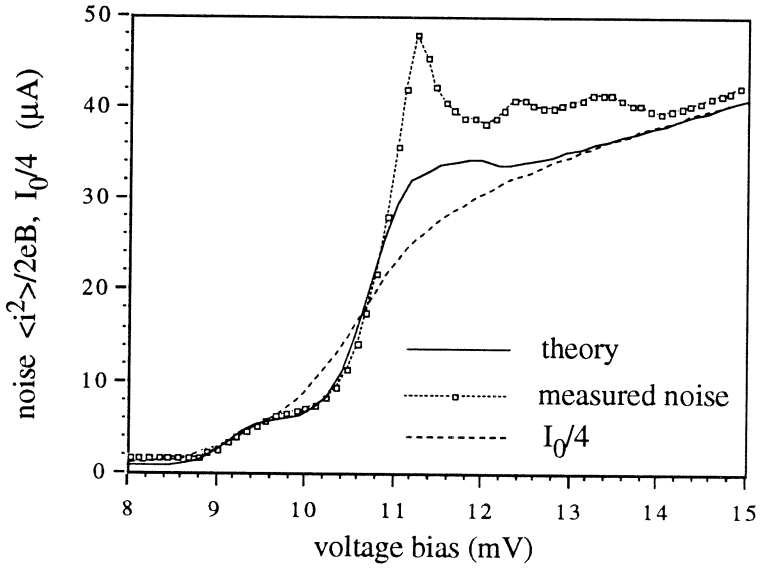

Figure 7 Photon induced noise in a four junction series array as a function of the bias voltage. Also plotted is the measured dc current divided by the number of junctions in the array, for comparison to shot noise. The rf power power corresponds to $\alpha = 1.0$ at 9.87 mV and rf frequency is 95.5 GHz.

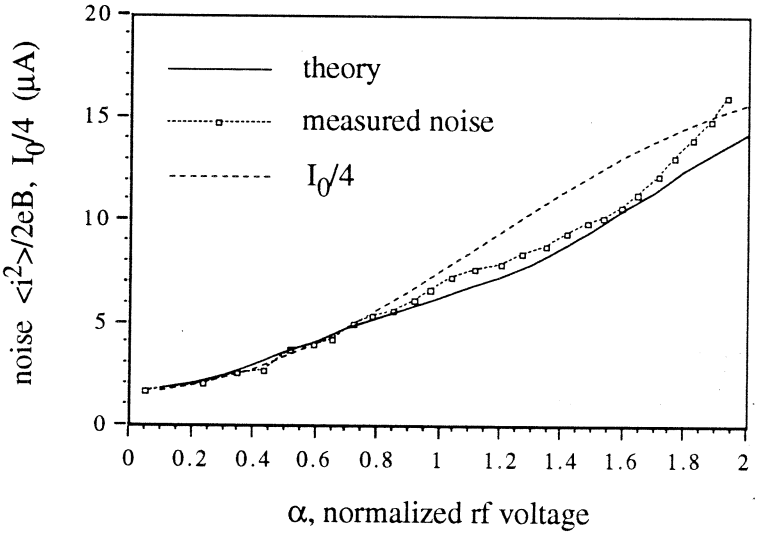

Figure 8 Photon induced noise in a four junction series array as a function of normalized rf voltage. The array was biased on its first photon step at 9.87 mV. Also plotted is the measured dc current divided by the number of junctions in the array, for comparison to shot noise.

junction" approach developed by Feldman and Rudner [11], assuming that the noise from each junction adds incoherently. Thus agreement of measurement with the theory verifies that the noise in the photon induced currents in each junction of an SIS array add independently. Incoherent addition of noise implies that the SIS mixer noise is independent of the number of junctions. Thus our measurements are in agreement with measurements done by Crété *et al.* [14] which showed that mixer noise in SIS arrays showed no significant dependence on the number of junctions for large $\omega R_n C$.

(iii) IBM single junction with tuning circuit

The photon induced noise measured for this junction is shown in figures 9 and 10. The measured noise shows very poor agreement with theory. As seen from figure 9 the theory underestimates the noise on the first photon step and overestimates the noise on the second photon step. The measured noise is about 1.6 times that predicted by theory in the middle of the first photon step at about 2.7 mV. In figure 10 we see that the deviation of measured noise from the theory, on the first photon step, gets more significant as the rf power increases.

This junction had an excellent IV curve that was very similar to the single Hypres junction as was shown in figure 3(a) and (b). However it's $\omega R_n C$ product was about half that of the Hypres junction and the integrated tuning circuit further improved the rf coupling. Thus it had a different source impedance which produced different theoretical noise. But the theory did not agree with our measurement. This seems to indicate that Tucker's noise theory works well for junctions with large $\omega R_n C$ and low rf coupling, but does not work well for small $\omega R_n C$ junctions or strong rf coupling.

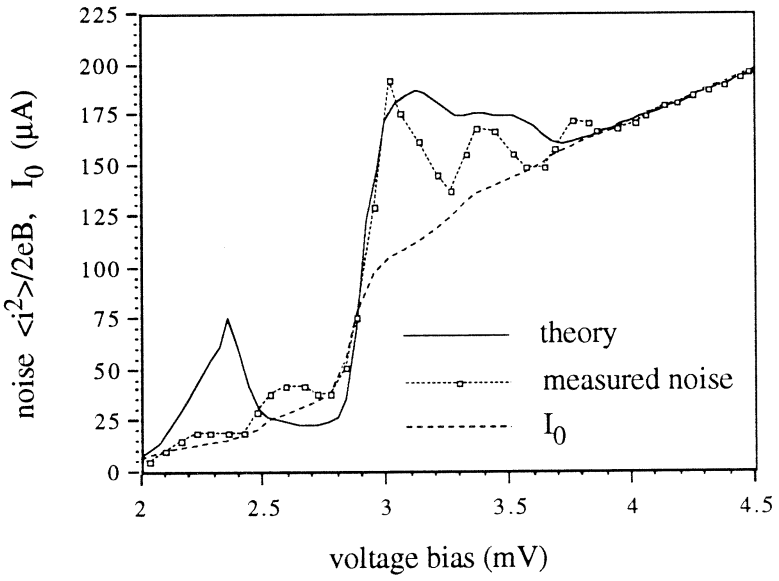

Figure 9 Photon noise in single IBM junction as a function of the voltage bias. The rf power corresponded to $\alpha = 1.10$ at 2.68 mV. The rf frequency is 95.5 GHz. Also plotted is the measured dc current, for comparison to shot noise.

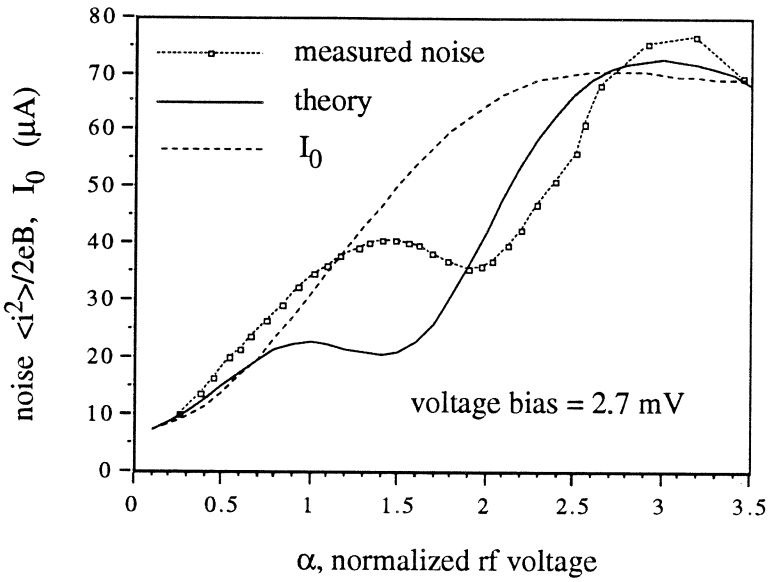

Figure 10 Photon induced noise in the single IBM junction as a function of normalized rf voltage. The junction was biased on the first step at 2.7 mV. Also shown is the measured dc current, for comparison to shot noise.

(iv) Hypres junction with tuning circuit

In order to verify that this deviation from theory was not dependent on the fabrication process, we also measured the photon induced noise in a Hypres junction with an integrated tuning circuit that was similar to the IBM junction. We could not bias stably on the first photon step of this junction, due to the very large or negative dynamic impedance in that region. However the noise measured on the second step was significantly less than that predicted by theory just as in the IBM junction.

Conclusions

We have built a very accurate system for measuring the amplitude of noise current sources in SIS junctions built in niobium mixer circuits. We have verified the accuracy of this system by measuring Johnson noise from the SIS at various temperatures above its superconducting transition.

We have experimentally verified that Tucker's theory of noise in SIS mixers [2] accurately predicts the output noise of SIS junctions with no radiation present, and that this noise is simply shot noise in the dc current of the SIS. Further, we have experimentally verified that Tucker's theory, combined with a vacuum noise term due to Wengler and Woody [3], is accurate for SIS junctions which are poorly coupled to a 95 GHz radiation field.

We have experimentally determined that the noise in arrays of two and four SIS junctions are not mutually coherent. This verifies the "equivalent single junction" model of Feldman *et al.* [11]. It is consistent with an SIS mixer temperature which is independent of N, the number of SIS's in the array, as was found by Crété *et al.*[14]. Since we did the array measurement with high capacitance junctions, we cannot make a statement about low capacitance junctions which had higher mixer noise temperatures as N increased [14].

We have found that SIS mixers with tuning circuits which produce strong coupling to the 95 GHz radiation do not fit Tucker's noise theory for the three-port model. We have ruled out some simple reasons like a misestimate of the amount of thermal noise coupled to the SIS, and a misestimate of radiation coupling to the SIS. We find that the measured noise is higher than theory predicts by about 60% on the first photon step below the gap. This may account for the higher than theoretical mixer temperatures which are often measured in well coupled SIS mixers.

We intend to extend this work in two main directions. First, we are constructing a system to do photon injection measurements at 490 GHz to see if the interaction with these more energetic photons yields any different results. Second, we will measure the noise currents of SIS's at low frequencies to determine if there are 1/f components in SIS noise.

Acknowledgement

This work was supported by NASA grant NAGW-2510. We are grateful for superconducting niobium integrated circuits fabricated for us at Hypres in Elmsford, NY and at IBM in Yorktown Heights, NY.

References

1. Wengler, M.J., "Submillimeter wave detection with superconducting tunnel diodes," *Proc. IEEE,* vol. 80, pp. 1810-1826, November, 1992.

2. Tucker, J.R. and M.J. Feldman, "Quantum detection at millimeter wavelengths," *Rev. Mod. Phys.,* vol. 57, pp. 1055-1113, 1985.

3. Wengler, M.J. and D.P. Woody, "Quantum noise in heterodyne detection," *IEEE J. Quantum Electron.,* vol. QE-23, pp. 613-622, May, 1987.

4. McGrath, W.R., P.L. Richards, D.W. Face, D.E. Prober, and F.L. Lloyd, "Accurate experimental and theoretical comparisons between superconductor-insulator-superconductor mixers showing weak and strong quantum effects," *J. Appl. Phys.,* vol. 63, pp. 2479-2491, 1988.

5. Mears, C.A., Q. Hu, P.L. Richards, A.H. Worsham, D.E. Prober, and A.V. Räisänen, "Quantum limited quasiparticle mixers at 100 GHz," *IEEE Trans. Magn.,* vol. 27, pp. 3363-3369, March, 1991.

6. Winkler, D., N.G. Ugras, A.H. Worsham, D.E. Prober, N.R. Erickson, and P.F. Goldsmith, "A full-band waveguide SIS receiver with integrated tuning for 75-110 GHz," *IEEE Trans. Magn.,* vol. 27, pp. 2634-2637, March, 1991.

7. McGrath, W.R., A.V. Räisänen, and P.L. Richards, "Variable-temperature loads for use in accurate noise measurements of cryogenically-cooled microwave amplifiers and mixers," *Int. J. of IR and MM Waves,* vol. 7, pp. 543-553, April, 1986.

8. Pan, S.-K., A.R. Kerr, M.J. Feldman, A.W. Kleinsasser, J.W. Stasiak, R.L. Sandstrom, and W.J. Gallagher, "An 85-116 GHz SIS receiver using inductively shunted edge-junctions," *IEEE Trans. Microwave Theory Tech.,* vol. 37, pp. 580-592, March, 1989.

9. Pance, G. and M.J. Wengler. "Integrated tuning elements for millimeter and submillimeter SIS mixers," in *IEEE MTT-S.* Albuquerque: June 1-5, 1992.

10. Rogovin, D. and D.J. Scalapino, "Fluctuation phenomena in tunnel junctions," *Annals of Physics,* vol. 86, pp. 1-90, July, 1974.

11. Feldman, M.J. and S. Rudner, "Mixing with SIS arrays," in *Reviews of Infrared and Millimeter Waves,* K.J. Button, Editor. 1983, Plenum: New York. p. 47-75.

12. Woody, D.P., R.E. Miller, and M.J. Wengler, "85-115 GHz receivers for radio astronomy," *IEEE Trans. Microwave Theory Tech.,* vol. MTT-33, pp. 90-95, February, 1985.

13. Tucker, J.R., "Quantum limited detection in tunnel junction mixers," *IEEE J. Quantum Electron.,* vol. QE-15, pp. 1234-1258, November, 1979.

14. Crété, D.-G., W.R. McGrath, P.L. Richards, and F.L. Lloyd, "Performance of arrays of SIS junctions in heterodyne mixers," *IEEE Trans. Microwave Theory Tech.,* vol. MTT-35, pp. 435-440, April, 1987.